ACCOUNTS of chemical research

Article

pubs.acs.org/accounts

Na-Ion Battery Anodes: Materials and Electrochemistry

Wei Luo,[†,‡] Fei Shen,[†] Clement Bommier,[§] Hongli Zhu,[†] Xiulei Ji,[*,§] and Liangbing Hu[*,†]

[†]Department of Materials Science and Engineering and [‡]Department of Mechanical Engineering, University of Maryland, College Park, Maryland 20742, United States

[§]Department of Chemistry, Oregon State University, Corvallis, Oregon 97331, United States

CONSPECTUS: The intermittent nature of renewable energy sources, such as solar and wind, calls for sustainable electrical energy storage (EES) technologies for stationary applications. Li will be simply too rare for Li-ion batteries (LIBs) to be used for large-scale storage purposes. In contrast, Na-ion batteries (NIBs) are highly promising to meet the demand of grid-level storage because Na is truly earth abundant and ubiquitous around the globe. Furthermore, NIBs share a similar rocking-chair operation mechanism with LIBs, which potentially provides high reversibility and long cycling life. It would be most efficient to transfer knowledge learned on LIBs during the last three decades to the development of NIBs. Following this logic, rapid progress has been made in NIB cathode materials, where layered metal oxides and polyanionic compounds exhibit encouraging results. On the anode side, pure graphite as the standard anode for LIBs can only form NaC_{64} in NIBs if solvent co-intercalation does not occur due to the unfavorable thermodynamics. In fact, it was the utilization of a carbon anode in LIBs that enabled the commercial successes. Anodes of metal-ion batteries determine key characteristics, such as safety and cycling life; thus, it is indispensable to identify suitable anode materials for NIBs.

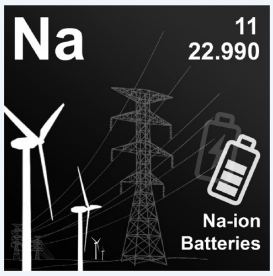

In this Account, we review recent development on anode materials for NIBs. Due to the limited space, we will mainly discuss carbon-based and alloy-based anodes and highlight progress made in our groups in this field. We first present what is known about the failure mechanism of graphite anode in NIBs. We then go on to discuss studies on hard carbon anodes, alloy-type anodes, and organic anodes. Especially, the multiple functions of natural cellulose that is used as a low-cost carbon precursor for mass production and as a soft substrate for tin anodes are highlighted. The strategies of minimizing the surface area of carbon anodes for improving the first-cycle Coulombic efficiency are also outlined, where graphene oxide was employed as dehydration agent and 2,2,6,6-tetramethylpiperidine-1-oxyl (TEMPO) was used to unzip wood fiber. Furthermore, surface modification by atomic layer deposition technology is introduced, where we discover that a thin layer of Al_2O_3 can function to encapsulate Sn nanoparticles, leading to a much enhanced cycling performance. We also highlight recent work about the phosphorene/graphene anode, which outperformed other anodes in terms of capacity. The aromatic organic anode is also studied as anode with very high initial sodiation capacity. Furthermore, electrochemical intercalation of Na ions into reduced graphene oxide is applied for fabricating transparent conductors, demonstrating the great feasibility of Na ion intercalation for optical applications.

1. INTRODUCTION

Over the past three decades, Li-ion batteries (LIBs) have achieved tremendous success as power sources for portable electronic devices and electric vehicles (EVs). However, technological improvement of LIBs cannot address the rarity of Li resources, which may lead to a risk that EVs powered by LIBs will no longer be affordable with their exhaustive usage.[1] Thus, it is critical to develop alternative battery technologies beyond LIBs based on earth abundant elements. One highly promising candidate is Na, which is adjacent to Li on the periodic table. It shares many similar alkali metal chemistries with Li and is very abundant and widely distributed.[1−3] The concept of Na-ion batteries (NIBs) is not new: they were investigated together with LIBs back in the 1980s;[4] however, by the early 1990s, the research community quickly lost interest in NIBs due to the lower energy density of NIBs and the advance of LIBs.

Recently, ambient-temperature NIBs have raised much attention again for grid-level applications considering the sustainability advantages of NIBs. Significant progress has been made for NIB cathodes by adapting the knowledge learned on LIBs.[5,6] As for anode materials, graphite, the commercial anode for LIBs, does not function in NIBs due to its extremely low capacity. This can be alleviated with solvent co-intercalation, but such a method brings about its own set of challenges.[7] Therefore, numerous attempts have been made to find suitable anodes for NIBs.

Although there have been several review articles related to NIB anodes,[8−10] this Account aims to summarize recent progresses made in carbon based and alloy based anodes for NIBs, especially from our research groups. We will highlight high performance hard carbon anodes and new insights on the Na ion storage mechanism in hard carbon. We will then discuss alloying type anodes, such as tin (Sn) and phosphorus (P), which demonstrate some of the highest reported capacities but have their own unique set of challenges and solutions. Lastly, metal oxides, sulfides, and organic based anodes will be reviewed, albeit briefly due to the limited space.

Received: October 27, 2015
Published: January 19, 2016

DOI: 10.1021/acs.accounts.5b00482
Acc. Chem. Res. 2016, 49, 231−240

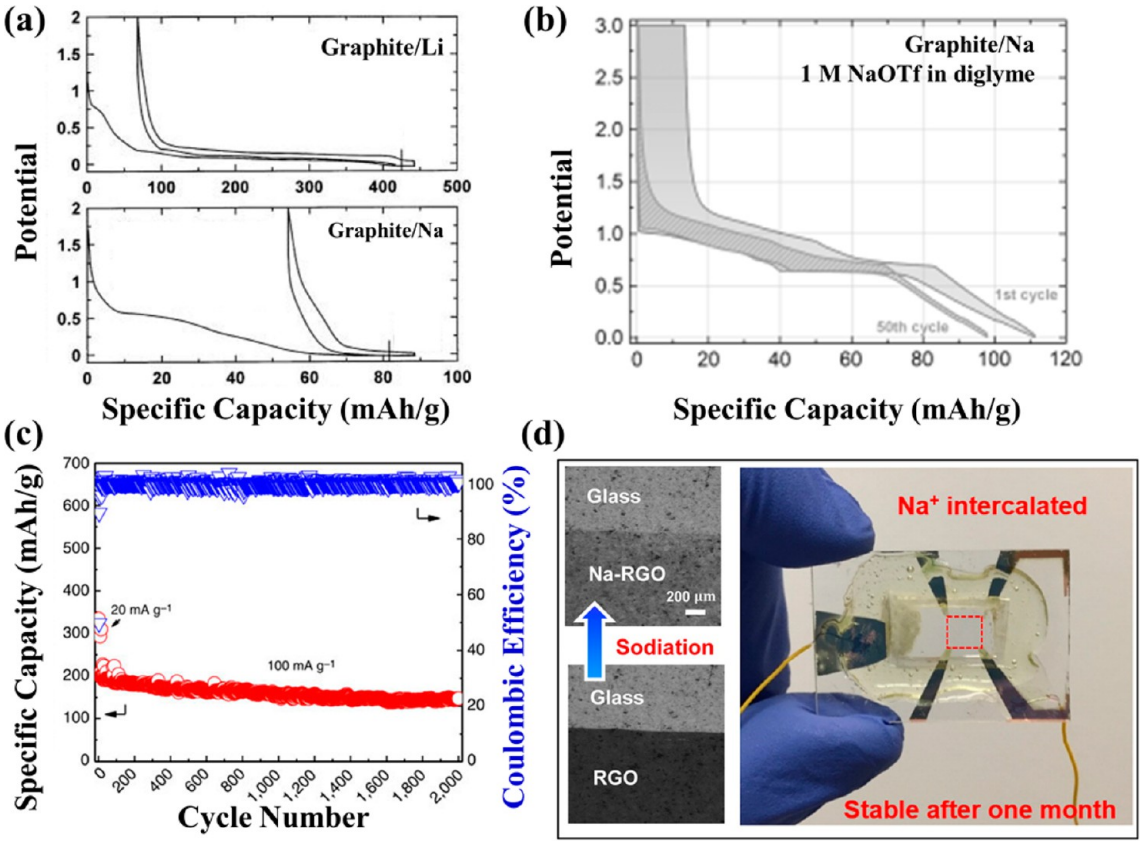

Figure 1. (a) Potential profiles of graphite electrodes in LIBs and NIBs.[26] Reproduced by permission of The Electrochemical Society. (b) Co-intercalation of Na ion and diglyme into graphite in NIBs. Reproduced from ref 7. Copyright 2014 WILEY. (c) Superior cycling performance of expanded graphite anode in NIBs. Reprinted by permission from Macmillan Publishers Ltd: *Nat. Commun.* (ref 19), copyright 2014. (d) Na ion intercalation into RGO enables a transparent conductor. Reproduced from ref 25. Copyright 2015 American Chemical Society.

2. CARBON ANODES

Carbon based anodes are leading candidates for LIBs due to their low potential, high capacity, abundance, and low cost.[11] For the same reasons, carbon anodes are also among the most promising choices for NIBs.

2.1. Graphitic Carbon

Li ions are readily inserted into graphite with a final stoichiometry of LiC_6, which is equivalent to a capacity of 372 mA·h/g. However, only a small amount of Na atoms can be intercalated into graphite (Figure 1a).[12,13] This limited capacity can be explained from a thermodynamic perspective, which is associated with Na plating on the carbon surface before forming the graphite intercalation compounds (GICs).[14−16] For example, Grande et al. performed a density functional theory (DFT) study and calculated the binding energy between Li, Na, K, and graphene sheets, which showed that NaC_6 was the only intercalation compound that was not energetically favorable.[14] Furthermore, solvation energy plays a significant role in the feasibility of intercalation, though this has yet to be comprehensively studied.

Recently, Adelhelm et al. proposed a co-intercalation approach to form a Na−solvent−graphite ternary GIC anode for NIBs.[7] With use of a diglyme-based electrolyte, graphite exhibited a reversible capacity of ∼100 mA·h/g with a potential plateau at 0.6 V at 0.1 C (Figure 1b). Such an unexpected capacity is due to a co-intercalation of diglyme solvated Na ions into graphite. Recently, Kang's group further developed an ether-based electrolyte for graphite anodes.[17] However, co-intercalation of solvents causes a high level of volume change, inherently limiting its practical application.

Another approach to utilize graphitic carbons is to expand their interlayer distance.[18−20] For example, Wang's group reported an expanded graphite anode with an interlayer distance of 0.43 nm.[19] The as-obtained expanded graphite shows a high reversible capacity of ∼300 mA·h/g at 20 mA/g and a stable performance for 2000 cycles (Figure 1c). By comparing various reduction conditions, Singh demonstrated that increasing order and decreasing interlayer spacing of reduced graphene oxide (RGO) lead to a poorer performance.[20] Recently, Mitlin and co-workers produced graphene-like materials from peat moss, which exhibited enlarged intergraphene spacing (0.388 nm) and promising Na ion storage properties.[21] Ji and co-workers also discovered that a narrower interlayer spacing of graphitizable carbon leaded to a lower capacity.[22]

On the other hand, Na ion or Li ion intercalation can be used to tune the properties of two-dimensional (2D) materials.[23,24] For example, Wang et al. reported that Li ion intercalation can effectively tune the structure and properties of MoS_2. They demonstrated that lithiated MoS_2 exhibited an enhanced hydrogen evolution reaction activity. Inspired by this, for the first time, we have successfully applied the electrochemical intercalation of Na ions to build a transparent electrode.[25] As shown in Figure 1d, printed RGO films become much more transparent after intercalation of Na ions (from 36% to 79%). Meanwhile, the sheet resistance shows a 270 times decrease (from 83 000 to 311 Ω/sq), which is attributed to the

DOI: 10.1021/acs.accounts.5b00482
Acc. Chem. Res. 2016, 49, 231−240

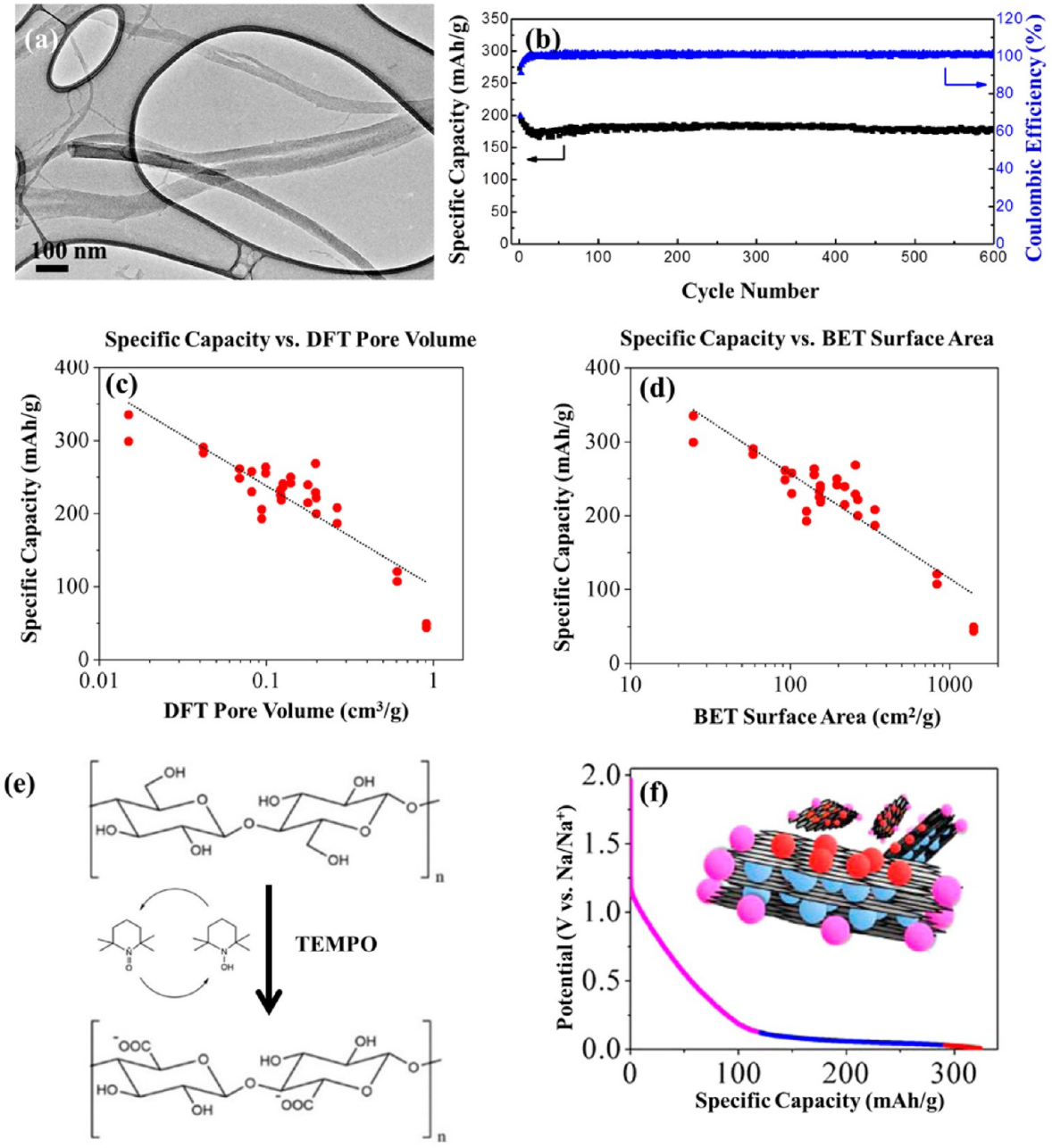

Figure 2. (a, b) Cellulose nanofiber derived CNFs as a long-life NIB anode. Reproduced from ref 31 with permission from The Royal Society of Chemistry. (c, d) Specific capacity as a function of DFT pore volume and BET surface area. Reprinted from ref 34, with permission from Elseiver. (e) Mechanism of treating cellulose by TEMPO. Adapted from ref 40. Copyright 2015 American Chemical Society. (f) A three-tiered mechanism for Na ion storage in hard carbon anode. Reproduced from ref 42. Copyright 2015 American Chemical Society.

enhancement of carrier density in RGO and better contact between RGO layers by Na ion intercalation.

2.2. Hard Carbon

Hard carbon, also known as non-graphitizable carbon, cannot be graphitized by thermal treatment.[11] In 2000, Stevens and Dahn demonstrated that glucose-derived hard carbon exhibits a desodiation capacity of ~300 mA·h/g.[26,27] Inspired by their pioneering work, there have been many reports on hard carbon anodes.[28−30] Luo et al. studied the impact of morphology on cycling performance of hard carbon, where carbon nanofibers derived from cellulose exhibited a stable capacity of 176 mA·h/g at 200 mA/g over 600 cycles (Figure 2a,b).[31] Similar performance is also demonstrated in other one-dimensional (1D) hard carbon anodes.[32,33] Note that it is still elusive whether the stable cycling is directly linked to the 1D morphology or the shorter ion diffusion distance and enhanced stress tolerance.

Ji's group then studied the correlation between the open nanoporosity and the specific capacity of hard carbon anodes, where Bommier et al. found that increased surface area via CO_2 activation led to lower reversible capacity (Figure 2c,d).[34] Furthermore, porous carbon anodes typically exhibit very low first-cycle Coulombic efficiency (FCCE),[35,36] which is a serious issue. Noticeably, the low capacity and poor FCCE is caused by the more prominent formation of a solid electrolyte interphase (SEI) layer on the large surface area.[37,38]

DOI: 10.1021/acs.accounts.5b00482
Acc. Chem. Res. 2016, 49, 231−240

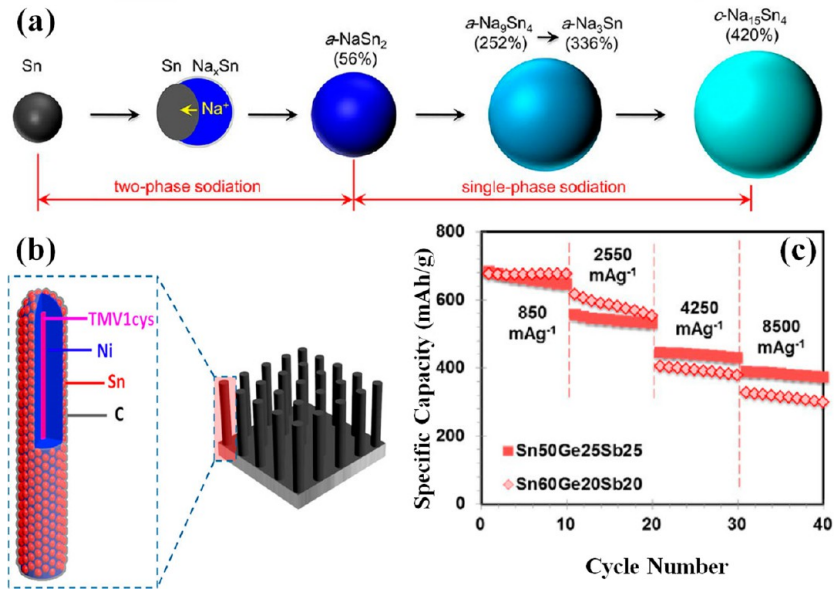

Figure 3. (a) The structural evolution of Sn anode upon sodiation. Reproduced from ref 45. Copyright 2012 American Chemical Society. (b) Depositing Sn nanoparticles onto a 3D Ni-coated tobacco mosaic virus (TMV) as anodes for NIBs. Reproduced from ref 46. Copyright 2013 American Chemical Society. (c) Optimizing ternary Sn/Ge/Sb thin film alloys as anodes for NIBs. Reproduced from ref 49. Copyright 2014 American Chemical Society.

The results related to surface area motivated us to minimize the surface area of hard carbon anodes. Luo et al. employed GO as a 2D dehydration agent to prevent foaming during caramelization of sucrose, which extends the burnoff duration of sucrose caramel over a wider temperature range.[39] Accordingly, the specific surface area of the resulting carbon reduces from 137.2 to 5.4 m^2/g, and the FCCE is improved from 74% to 83%. To increase FCCE, Hu's group discovered that pretreating cellulose fiber with 2,2,6,6-tetramethylpiperidine-1-oxyl (TEMPO) before thermal carbonization can reduce surface area from 586 to 126 m^2/g.[40] This is made possible because TEMPO can unzip the cellulose fibers by oxidizing hydroxyl groups to carboxyl groups, thus loosening the hydrogen bond (Figure 2e). After the paper-making process, the flat structure of ribbon-like TEMPO-treated fiber results in a much denser paper and leads to the lower surface area after carbonization. FCCE is greatly enhanced from 28% to 72%, and a stable cycling performance of 200 mA·h/g at 100 mA/g for 200 cycles is obtained.

It has been widely believed that Na ion storage in hard carbon follows the sequential intercalation into turbostratic nanodomains (TNs) and pore filling into the voids between TNs.[26] This model is known as the "card-house" model supported by experimental evidence; however, some recent experimental results showed discrepancies. For example, Cao et al. proposed that Na ion intercalation into the TNs of hollow carbon nanowires corresponds to the potential plateau at low potentials.[30] Moreover, *ex situ* XRD by both Komaba et al. and Mitlin et al. showed a reversible dilation and contraction of the TNs in the low voltage plateau.[21,29,41] Recently, Bommier et al. suggested that the storage mechanism may be three tiered, where the sloping capacity was assigned to defect sites, supported by *ex situ* total neutron scattering/associated pair distribution function (PDF) studies (Figure 2f).[42] From galvanostatic intermittent titration technique (GITT), the authors observed a substantial increase in diffusivity at voltages close to Na metal plating, which breaks the plateau region down to two possible storage mechanisms. Certainly, further studies are demanded to fully understand the mechanisms of Na storage in hard carbon, particularly for the plateau region.

3. ALLOY ANODES

Alloy-type anodes are attractive for their high capacities in NIBs. However, the large volume change of alloy anodes upon electrochemical cycling may cause electrode pulverization, loss of contact with the current collector, and consequent capacity fading.[43] To tackle this problem, several strategies such as using smart substrates, fabricating nanostructures, and using special binder have been developed.

3.1. Tin

By forming $Na_{15}Sn_4$, Sn exhibits a high theoretical capacity of 847 mA·h/g.[44] In 2012, Huang et al. discovered that Sn initially forms the Na_xSn ($x \approx 0.5$) phase, which converts to its final $Na_{15}Sn_4$ structure.[45] With coupling with *in situ* transmission electron microscopy (TEM) technology, they proved that Na_xSn ($x \approx 0.5$) and $Na_{15}Sn_4$ correspond to 60% and 420% volumetric expansion (Figure 3a). To overcome the impact of volume change, Wang et al. coated Sn onto three-dimensional (3D) current collectors with nickel nanofibers, which are later covered by carbon and greatly improved cycling (Figure 3b).[46] Additionally, it has been suggested that optimizing binder or components plays a critical role in Sn based anodes.[47−49] For example, $Sn_{50}Ge_{25}Sb_{25}$ exhibits high capacity (833 mA·h/g at 85 mA/g), excellent rate capability (381 mA·h/g at 8500 mA/g), and stable cycling performance (662 mA·h/g after 50 cycles at 85 mA/g) (Figure 3c).[49]

For improving cycling performance of Sn anodes, Hu's group has contributed two new strategies. The first involves a hierarchical wood fiber substrate, which yields a stable cycling performance over 400 cycles.[50] With performing experiment and continuum chemomechanical modeling, we discovered that the soft texture of wood fiber can effectively buffer the mechanical stresses of Sn anode upon alloying/dealloying. In addition, the porous nature of the substrate functions as an electrolyte

DOI: 10.1021/acs.accounts.5b00482
Acc. Chem. Res. 2016, 49, 231−240

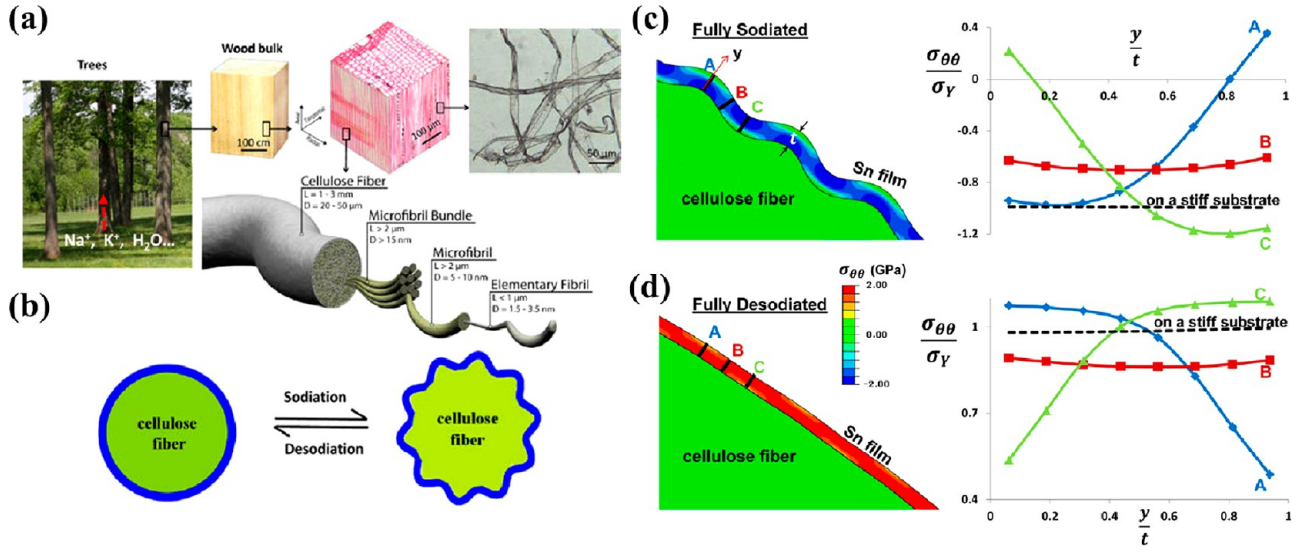

Figure 4. Wood fiber substrates are applied for Sn anode: (a) hierarchical structure of wood fiber; (b) structural wrinkling of wood fiber effectively releases sodiation generated stresses; (c, d) chemomechanical modeling of the hoop stresses in Sn@wood fiber anode at the fully sodiated (c) and desodiated (d) state. Reproduced from ref 50. Copyright 2013 American Chemical Society.

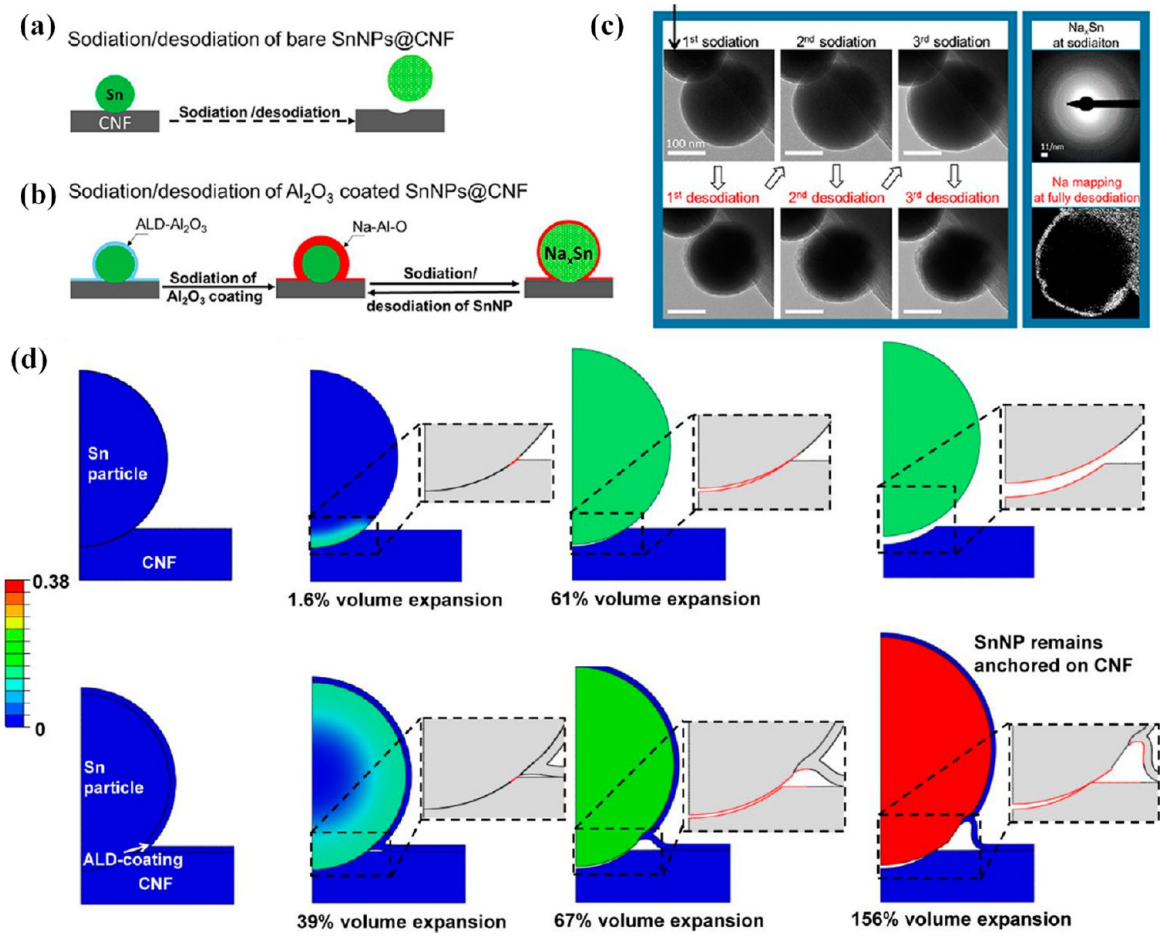

Figure 5. ALD technology is employed for improving the cycling performance of Sn anodes: (a, b) comparison of bare Sn and ALD-Al_2O_3 coated Sn nanoparticle on carbon nanofiber; (c) *in situ* TEM images of the first three cycles; (d) FEM modeling. Reproduced from ref 51. Copyright 2014 American Chemical Society.

reservoir that enables dual ion transportation through the substrate (Figure 4). Aside from substrate selection, surface modification of Sn anode with an atomic layer deposition (ALD) Al_2O_3 coating remarkably boosts the cycling performance.[51] With *in situ* TEM, we unveiled the dynamic mechanical protection of the ALD-Al_2O_3 coating by coherently deforming

DOI: 10.1021/acs.accounts.5b00482
Acc. Chem. Res. 2016, 49, 231−240

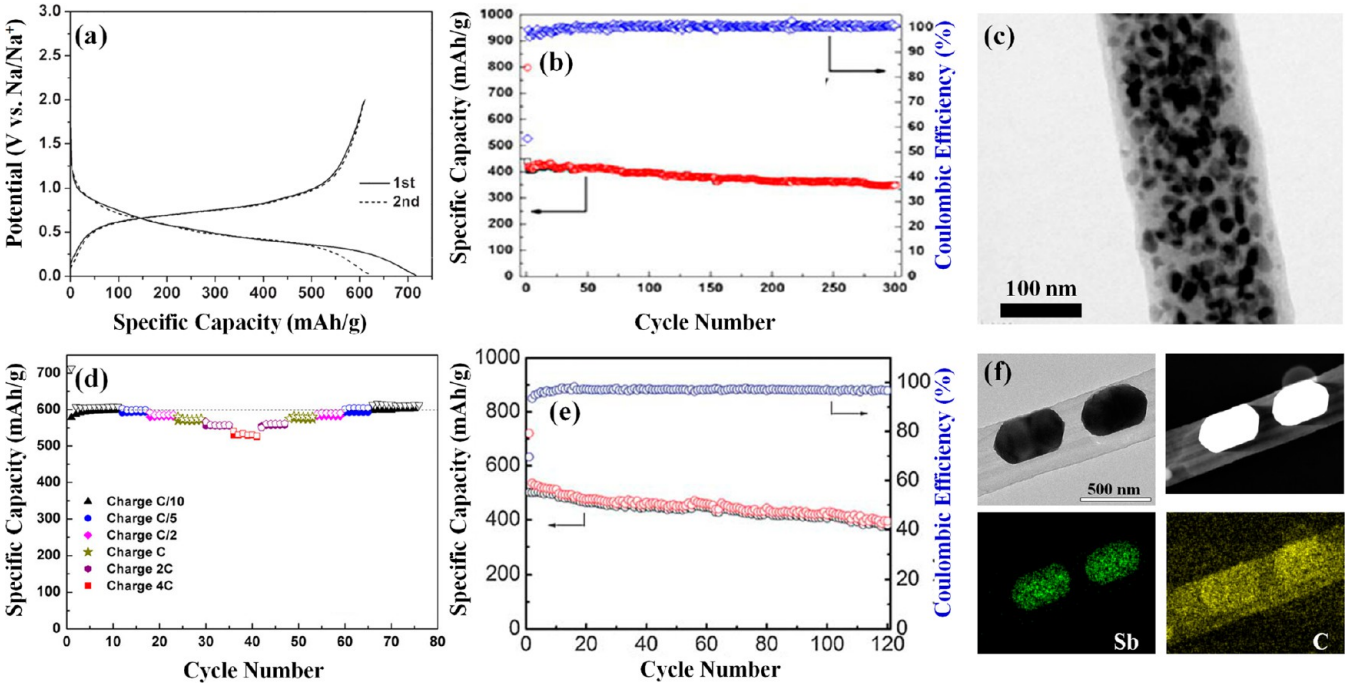

Figure 6. (a) Potential profiles of Sb/C composite. Reproduced from 52 with permission of The Royal Society of Chemistry. (b, c) Cycling performance and TEM image of Sb nanofiber. Reproduced from ref 56. Copyright 2013 American Chemical Society. (d) Rate capability of Sb electrode with vapor ground carbon fibers as the conductive additive and carboxymethyl cellulose binder. Adapted from ref 57. Copyright 2012 American Chemical Society. (e) Cycling performance and CE of Sb/CNT composites. Reproduced from ref 58 with permission of The Royal Society of Chemistry. (f) One-dimensional peapod-like Sb@C sub-micrometer structures. Reproduced from ref 60 with permission from the Royal Society of Chemistry.

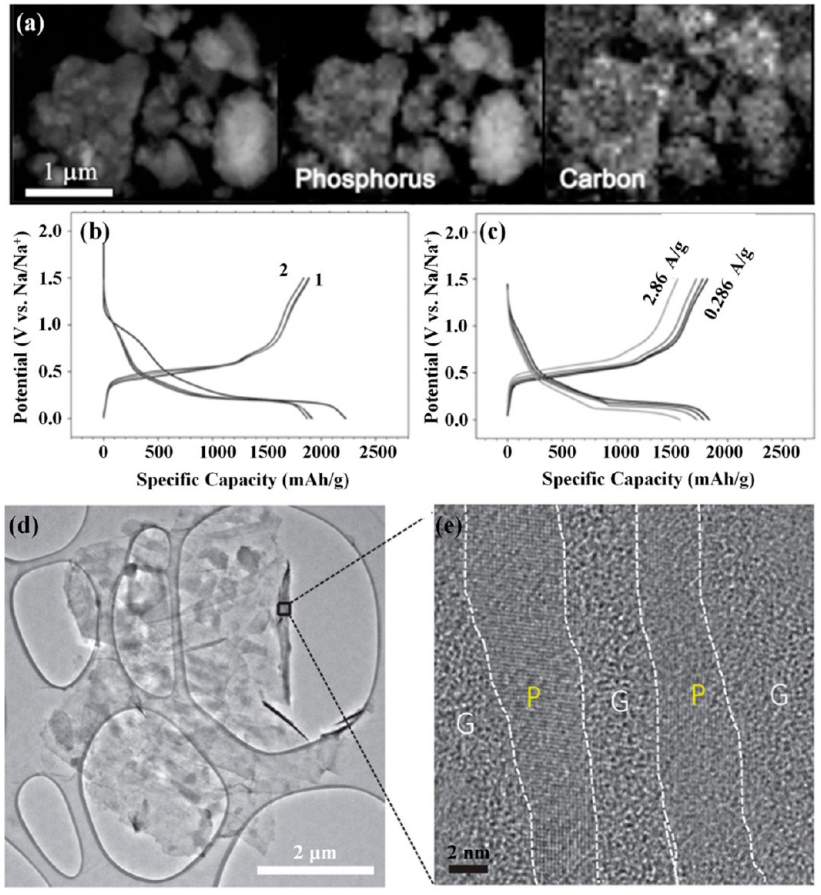

Figure 7. (a–c) Ball-milling red P/carbon composite as an anode for NIBs. Reproduced with permission from ref 62. Copyright 2013 WILEY. (d, e) Phosphorene–graphene anodes. Reprinted by permission from Macmillan Publishers Ltd: *Nat. Nanotechnol.* (ref 66), copyright 2015.

DOI: 10.1021/acs.accounts.5b00482
Acc. Chem. Res. 2016, 49, 231–240

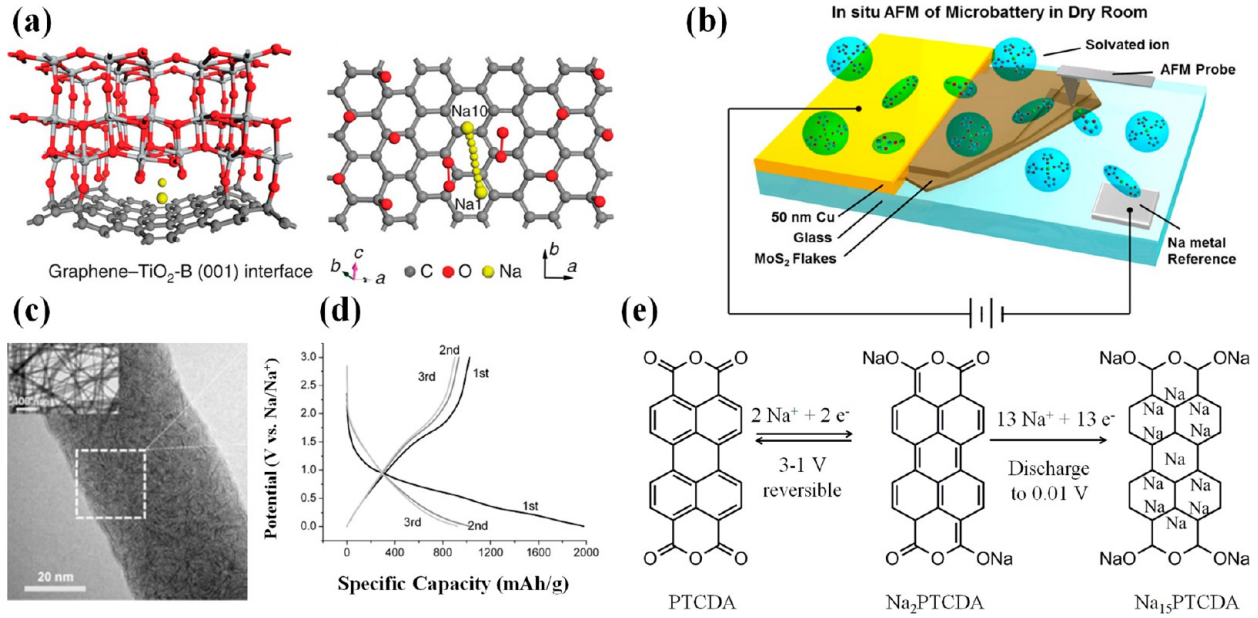

Figure 8. (a) First-principle calculations illustrate the Na diffusion path along the [010] direction of TiO_2 from Na1 to Na10 sites. Reprinted by permission from Macmillan Publishers Ltd: *Nat. Commun.* (ref 75), copyright 2015. (b) Planar microscale battery for *in situ* AFM measurements on MoS_2 electrode. Reproduced from ref 81. Copyright 2015 American Chemical Society. (c) Morphology of MoS_2 nanoplates embedded in carbon nanofibers and (d) corresponding potential profiles. Reproduced from ref 82. Copyright 2014 WILEY. (e) Electrochemical reactions between Na ions and PTCDA. Reproduced from ref 87. Copyright 2014 WILEY.

with Sn nanoparticle under the huge volume changes upon alloying/dealloying. Chemomechanical simulations clearly showed that bare Sn nanoparticles become disconnected from the underlying substrate upon charging. By contrast, the ALD-Al_2O_3 coating acts as ion-conductive nanoglue and robustly anchors the Sn nanoparticle anode to the substrate, thereby effectively enhancing the cyclability (Figure 5).

3.2. Antimony

Yang et al. first reported an Sb/C composite by ball-milling commercially available Sb particles with carbon black.[52] After ball-milling, bulk Sb particles become fine Sb nanocrystalline particles embedded in the carbon matrix. Such an Sb/C composite structure shows a reversible capacity as high as 610 mA·h/g at 100 mA/g, close to the full formation of Na_3Sb (660 mA·h/g, Figure 6a). To further improve the rate capability and cycling performance of the Sb anode, designing and fabricating nanostructures[53−56] and optimizing electrode components[57−59] have been widely used (Figure 6b−e). An interesting 1D peapod-like Sb@C structure with Sb sub-micrometer-particles encapsulated in carbon tubes has been developed by Luo et al. (Figure 6f).[60] The authors hoped that the void spaces could help buffer the volume change of Sb during alloying/dealloying, yet this morphology was not quite effective.

To further understand the structural and compositional evolution of the Sb anode upon sodiation/desodiation, Mitlin et al. developed an *in situ* electrochemical cell in TEM combining it with *ex situ* time-of-flight, secondary-ion mass spectrometry (TOFSIMS) depth profiling, and focused ion beam (FIB)−helium ion scanning microscope (HIM) imaging technologies.[61] They discovered that heterogeneous sodiation of Sb occurred, which resulted in major stresses. Their findings could shed light on commercialized micrometer-scale Sb particulates, which provides guidance for practical applications.

3.3. Phosphorus

P exhibits a theoretical capacity of ~2600 mA·h/g by forming Na_3P. Lee et al. and Yang et al. reported P anodes in NIBs at the same time.[62,63] They discovered that mechanical ball-milling of red P and carbon black at an optimized P/C ratio (7:3) leads to an amorphous P/C composite with great Na storage properties, including extremely high capacity (>2000 mA·h/g), excellent rate capability, and stable cycling performance (Figure 7a−c). Later, carbon nanotubes (CNTs)[64] and graphene[65] were also introduced into P electrodes, which showed comparable performance to amorphous P/C composites. Most recently, Cui et al. demonstrated a black P/graphene nanostructure, where they fabricated a sandwich-structure comprising a few phosphorene layers alternating with several graphene layers (Figure 7d,e).[66] This phosphorene/graphene structure delivers an extremely high capacity of 2440 mA·h/g at 50 mA/g and an 83% capacity retention for 100 cycles. They discovered that the graphene layers not only function as an electrical conductor but also serve as an elastic buffer for accommodating the volume expansion upon cycling.

Moreover, great progress has been achieved on other alloy anodes, including Ge[67,68] and Bi.[69] However, compared with Sn, Sb, or P, they are less promising due to the lower capacity or high cost. Furthermore, alloys or compounds also exhibit great performance.[49,70] Among them, facile ball-milling of Sn and P can result in an attractive NIB anode of Sn_4P_3.[71−73]

4. OTHER ANODES (METAL OXIDES/SULFIDES, ORGANIC MATERIALS)

Recently, many other anodes have also appeared, such as metal oxides, metal sulfides, and organic anodes. Previous reviews have covered these anode materials; thus, we briefly introduce several typical materials here.[1,8,9] Among metal oxides, TiO_2 is of considerable importance due to its promising performance, abundance, and low cost.[74] Recently, Chen et al. reported a

DOI: 10.1021/acs.accounts.5b00482
Acc. Chem. Res. 2016, 49, 231−240

TiO_2/graphene anode.[75] They demonstrated that pseudocapacitance occurred during Na ion intercalation, which enables high-rate capability (>90 mA·h/g at 36 C) and great stability over 4300 cycles (Figure 8a). Metal sulfides have also drawn great attention,[76−78] especially MoS_2.[79,80] To understand the evolving structural changes and the formation of SEI on MoS_2, Lacey et al. fabricated a microscale planar battery combined with an *in situ* atomic force microscopy (AFM) (Figure 8b).[81] We, for the first time, observed that a wrinkling behavior of mechanically exfoliated MoS_2 flakes occurs upon sodiation at 0.4 V, and the SEI forms quickly before the intercalation of Na ions. Moreover, AFM measurements suggested that the thickness of SEI on MoS_2 electrode is about 20.4 nm ± 10.9 nm. Among various MoS_2 electrodes, electrospun MoS_2 nanofibers show great promise.[82,83] For example, Yu et al. prepared an interesting structure of embedding single-layered MoS_2 nanoplates in carbon nanofibers, which delivers a high reversible Na ion storage capacity of 854 mA·h/g (Figure 8c,d).[82]

Additionally, organic materials have also been investigated as anodes for NIBs due to their low cost, designability, and recyclability.[84−86] Most recently, Luo et al. discovered that unmodified 3,4,9,10-perylene-tetracarboxylicacid-dianhydride (PTCDA) can deliver a significant Na ion storage capacity.[87] During sodiation of PTCDA, Na_{15}PTCDA with a high sodiation capacity of 1017 mA·h/g can be formed (Figure 8e).

5. CONCLUSIONS

In this Account, we mainly surveyed recent developments on carbon-based and alloy-based anodes for NIBs. Progress has been made on minimizing the surface area of hard carbon anodes for a higher FCCE. New insights on Na ion storage mechanism in hard carbon have also been proposed. Mixing alloy-type materials with carbon by mechanical ball milling provides a simple and effective strategy to produce high capacity anodes. Our soft substrate and ALD surface modification for tin anode open a new mind for this direction. Moreover, advanced characterization technologies, such as *in situ* TEM and *in situ* AFM have been conducted to investigate the fundamental electrochemistry for NIBs. Furthermore, Na ion intercalation has also been applied to fabricate transparent electrodes.

In summary, significant progress has been realized in the past few years for NIB anodes, but it is still in its early stage. In the short term, hard carbon may be the best choice for mass production of NIBs. High capacity anodes, such as alloying anodes, show great promise in the near future. Moreover, a Na metal anode may become the next research focus.

AUTHOR INFORMATION

Corresponding Authors

*E-mail: binghu@umd.edu.
*E-mail: david.ji@oregonstate.edu.

Notes

The authors declare no competing financial interest.

Biographies

Wei Luo is currently a Postdoctoral Researcher at University of Maryland, College Park. His research focuses on new materials and their properties for energy storage and conversion.

Fei Shen is a Ph.D. candidate at Nanjing University. He is currently visiting University of Maryland, College Park, as a joint Ph.D. student. His research focuses on Li/Na-ion batteries.

Clement Bommier is currently completing his Ph.D. studies at Oregon State University. His research focuses on carbon materials for energy storage and computational material science.

Hongli Zhu is currently an Assistant Professor in Northeastern University. Her group focuses on the research of energy storage, advanced manufacturing, and multifunctional materials.

Xiulei Ji is an Assistant Professor of Chemistry at Oregon State University. His group focuses on carbon-based materials in energy storage and conversion.

Liangbing Hu is an Assistant Professor in the energy research center of University of Maryland, College Park. He is leading a research group on energy storage and flexible electronics with a focus on nanomaterials.

ACKNOWLEDGMENTS

L. Hu acknowledges the support from Nanostructures for Electrical Energy Storage (NEES), an Energy Frontier Research Center funded by the U.S. Department of Energy, Office of Science, Basic Energy Sciences, under Award DESC0001160. We also are thankful for the support from NSF-CBET Grant 1335979. X. Ji acknowledges the support from National Science Foundation, Award number 1507391.

REFERENCES

(1) Yabuuchi, N.; Kubota, K.; Dahbi, M.; Komaba, S. Research development on sodium-ion batteries. *Chem. Rev.* **2014**, *114*, 11636−11682.
(2) Kim, S. W.; Seo, D. H.; Ma, X.; Ceder, G.; Kang, K. Electrode materials for rechargeable sodium-ion batteries: Potential alternatives to current lithium-ion batteries. *Adv. Energy Mater.* **2012**, *2*, 710−721.
(3) Slater, M. D.; Kim, D.; Lee, E.; Johnson, C. S. Sodium-ion batteries. *Adv. Funct. Mater.* **2013**, *23*, 947−958.
(4) Delmas, C.; Braconnier, J. J.; Fouassier, C.; Hagenmuller, P. Electrochemical intercalation of sodium in Na_xCoO_2 bronzes. *Solid State Ionics* **1981**, *3*−*4*, 165−169.
(5) Palomares, V.; Serras, P.; Villaluenga, I.; Hueso, K. B.; Carretero-Gonzalez, J.; Rojo, T. Na-ion batteries, recent advances and present challenges to become low cost energy storage systems. *Energy Environ. Sci.* **2012**, *5*, 5884−5901.
(6) Pan, H.; Hu, Y. S.; Chen, L. Room-temperature stationary sodium-ion batteries for large-scale electric energy storage. *Energy Environ. Sci.* **2013**, *6*, 2338−2360.
(7) Jache, B.; Adelhelm, P. Use of graphite as a highly reversible electrode with superior cycle life for sodium-ion batteries by making use of co-intercalation phenomena. *Angew. Chem., Int. Ed.* **2014**, *53*, 10169−10173.
(8) Dahbi, M.; Yabuuchi, N.; Kubota, K.; Tokiwa, K.; Komaba, S. Negative electrodes for Na-ion batteries. *Phys. Chem. Chem. Phys.* **2014**, *16*, 15007−15028.
(9) Kim, Y.; Ha, K. H.; Oh, S. M.; Lee, K. T. High-capacity anode materials for sodium-ion batteries. *Chem. - Eur. J.* **2014**, *20*, 11980−11992.
(10) Bommier, C.; Ji, X. L. Recent development on anodes for Na-ion batteries. *Isr. J. Chem.* **2015**, *55*, 486−507.
(11) Dahn, J. R.; Zheng, T.; Liu, Y.; Xue, J. S. Mechanisms for lithium insertion in carbonaceous materials. *Science* **1995**, *270*, 590−593.
(12) Metrot, A.; Guerard, D.; Billaud, D.; Herold, A. New results about the sodium-graphite system. *Synth. Met.* **1980**, *1*, 363−369.
(13) Ge, P.; Fouletier, M. Electrochemical intercalation of sodium in graphite. *Solid State Ionics* **1988**, *28*−*30* (Part 2), 1172−1175.
(14) Wang, Z.; Selbach, S. M.; Grande, T. Van der Waals density functional study of the energetics of alkali metal intercalation in graphite. *RSC Adv.* **2014**, *4*, 4069−4079.
(15) Okamoto, Y. Density functional theory calculations of alkali metal (Li, Na, and K) graphite intercalation compounds. *J. Phys. Chem. C* **2014**, *118*, 16−19.

DOI: 10.1021/acs.accounts.5b00482
Acc. Chem. Res. 2016, 49, 231−240

(16) Nobuhara, K.; Nakayama, H.; Nose, M.; Nakanishi, S.; Iba, H. First-principles study of alkali metal-graphite intercalation compounds. *J. Power Sources* **2013**, *243*, 585−587.
(17) Kim, H.; Hong, J.; Park, Y. U.; Kim, J.; Hwang, I.; Kang, K. Sodium storage behavior in natural graphite using ether-based electrolyte systems. *Adv. Funct. Mater.* **2015**, *25*, 534−541.
(18) Wang, Y. X.; Chou, S. L.; Liu, H. K.; Dou, S. X. Reduced graphene oxide with superior cycling stability and rate capability for sodium storage. *Carbon* **2013**, *57*, 202−208.
(19) Wen, Y.; He, K.; Zhu, Y.; Han, F.; Xu, Y.; Matsuda, I.; Ishii, Y.; Cumings, J.; Wang, C. Expanded graphite as superior anode for sodium-ion batteries. *Nat. Commun.* **2014**, *5*, 4033.
(20) David, L.; Singh, G. Reduced graphene oxide paper electrode: Opposing effect of thermal annealing on Li and Na cyclability. *J. Phys. Chem. C* **2014**, *118*, 28401−28408.
(21) Ding, J.; Wang, H.; Li, Z.; Kohandehghan, A.; Cui, K.; Xu, Z.; Zahiri, B.; Tan, X.; Lotfabad, E. M.; Olsen, B. C.; Mitlin, D. Carbon nanosheet frameworks derived from peat moss as high performance sodium ion battery anodes. *ACS Nano* **2013**, *7*, 11004−11015.
(22) Luo, W.; Jian, Z.; Xing, Z.; Wang, W.; Bommier, C.; Lerner, M. M.; Ji, X. Electrochemically expandable soft carbon as anodes for Na-ion batteries. *ACS Cent. Sci.* **2015**, *1*, 516.
(23) Wang, H.; Lu, Z.; Xu, S.; Kong, D.; Cha, J. J.; Zheng, G.; Hsu, P. C.; Yan, K.; Bradshaw, D.; Prinz, F. B.; Cui, Y. Electrochemical tuning of vertically aligned MoS_2 nanofilms and its application in improving hydrogen evolution reaction. *Proc. Natl. Acad. Sci. U. S. A.* **2013**, *110*, 19701−19706.
(24) Xiong, F.; Wang, H.; Liu, X.; Sun, J.; Brongersma, M.; Pop, E.; Cui, Y. Li intercalation in MoS_2: in situ observation of its dynamics and tuning optical and electrical properties. *Nano Lett.* **2015**, *15*, 6777−6784.
(25) Wan, J.; Gu, F.; Bao, W.; Dai, J.; Shen, F.; Luo, W.; Han, X.; Urban, D.; Hu, L. Sodium-ion intercalated transparent conductors with printed reduced graphene oxide networks. *Nano Lett.* **2015**, *15*, 3763−3769.
(26) Stevens, D. A.; Dahn, J. R. The mechanisms of lithium and sodium insertion in carbon materials. *J. Electrochem. Soc.* **2001**, *148*, A803−A811.
(27) Stevens, D. A.; Dahn, J. R. High capacity anode materials for rechargeable sodium-ion batteries. *J. Electrochem. Soc.* **2000**, *147*, 1271−1273.
(28) Thomas, P.; Billaud, D. Electrochemical insertion of sodium into hard carbons. *Electrochim. Acta* **2002**, *47*, 3303−3307.
(29) Komaba, S.; Murata, W.; Ishikawa, T.; Yabuuchi, N.; Ozeki, T.; Nakayama, T.; Ogata, A.; Gotoh, K.; Fujiwara, K. Electrochemical Na insertion and solid electrolyte interphase for hard-carbon electrodes and application to Na-ion batteries. *Adv. Funct. Mater.* **2011**, *21*, 3859−3867.
(30) Cao, Y.; Xiao, L.; Sushko, M. L.; Wang, W.; Schwenzer, B.; Xiao, J.; Nie, Z.; Saraf, L. V.; Yang, Z.; Liu, J. Sodium ion insertion in hollow carbon nanowires for battery applications. *Nano Lett.* **2012**, *12*, 3783−3787.
(31) Luo, W.; Schardt, J.; Bommier, C.; Wang, B.; Razink, J.; Simonsen, J.; Ji, X. Carbon nanofibers derived from cellulose nanofibers as a long-life anode material for rechargeable sodium-ion batteries. *J. Mater. Chem. A* **2013**, *1*, 10662−10666.
(32) Li, W.; Zeng, L.; Yang, Z.; Gu, L.; Wang, J.; Liu, X.; Cheng, J.; Yu, Y. Free-standing and binder-free sodium-ion electrodes with ultralong cycle life and high rate performance based on porous carbon nanofibers. *Nanoscale* **2014**, *6*, 693−698.
(33) Fu, L.; Tang, K.; Song, K.; van Aken, P. A.; Yu, Y.; Maier, J. Nitrogen doped porous carbon fibres as anode materials for sodium ion batteries with excellent rate performance. *Nanoscale* **2014**, *6*, 1384−1389.
(34) Bommier, C.; Luo, W.; Gao, W. Y.; Greaney, A.; Ma, S.; Ji, X. Predicting capacity of hard carbon anodes in sodium-ion batteries using porosity measurements. *Carbon* **2014**, *76*, 165−174.
(35) Tang, K.; Fu, L.; White, R. J.; Yu, L.; Titirici, M. M.; Antonietti, M.; Maier, J. Hollow carbon nanospheres with superior rate capability for sodium-based batteries. *Adv. Energy Mater.* **2012**, *2*, 873−877.
(36) Wang, H. G.; Wu, Z.; Meng, F. L.; Ma, D. L.; Huang, X. L.; Wang, L. M.; Zhang, X. B. Nitrogen-doped porous carbon nanosheets as low-cost, high-performance anode material for sodium-ion batteries. *ChemSusChem* **2013**, *6*, 56−60.
(37) Li, Y.; Xu, S.; Wu, X.; Yu, J.; Wang, Y.; Hu, Y. S.; Li, H.; Chen, L.; Huang, X. Amorphous monodispersed hard carbon micro-spherules derived from biomass as a high performance negative electrode material for sodium-ion batteries. *J. Mater. Chem. A* **2015**, *3*, 71−77.
(38) Memarzadeh Lotfabad, E.; Kalisvaart, P.; Kohandehghan, A.; Karpuzov, D.; Mitlin, D. Origin of non-SEI related Coulombic efficiency loss in carbons tested against Na and Li. *J. Mater. Chem. A* **2014**, *2*, 19685−19695.
(39) Luo, W.; Bommier, C.; Jian, Z.; Li, X.; Carter, R.; Vail, S.; Lu, Y.; Lee, J. J.; Ji, X. Low-surface-area hard carbon anode for Na-ion batteries via graphene oxide as a dehydration agent. *ACS Appl. Mater. Interfaces* **2015**, *7*, 2626−2631.
(40) Shen, F.; Zhu, H.; Luo, W.; Wan, J.; Zhou, L.; Dai, J.; Zhao, B.; Han, X.; Fu, K.; Hu, L. Chemically crushed wood cellulose fiber towards high-performance sodium-ion batteries. *ACS Appl. Mater. Interfaces* **2015**, *7*, 23291−23296.
(41) Ding, J.; Wang, H.; Li, Z.; Cui, K.; Karpuzov, D.; Tan, X.; Kohandehghan, A.; Mitlin, D. Peanut shell hybrid sodium ion capacitor with extreme energy-power rivals lithium ion capacitors. *Energy Environ. Sci.* **2015**, *8*, 941−955.
(42) Bommier, C.; Surta, T. W.; Dolgos, M.; Ji, X. New mechanistic insights on Na-ion storage in nongraphitizable carbon. *Nano Lett.* **2015**, *15*, 5888−5892.
(43) Chevrier, V. L.; Ceder, G. Challenges for Na-ion negative electrodes. *J. Electrochem. Soc.* **2011**, *158*, A1011−A1014.
(44) Li, Z.; Ding, J.; Mitlin, D. Tin and tin compounds for sodium ion battery anodes: Phase transformations and performance. *Acc. Chem. Res.* **2015**, *48*, 1657−1665.
(45) Wang, J. W.; Liu, X. H.; Mao, S. X.; Huang, J. Y. Microstructural evolution of tin nanoparticles during in situ sodium insertion and extraction. *Nano Lett.* **2012**, *12*, 5897−5902.
(46) Liu, Y.; Xu, Y.; Zhu, Y.; Culver, J. N.; Lundgren, C. A.; Xu, K.; Wang, C. Tin-coated viral nanoforests as sodium-ion battery anodes. *ACS Nano* **2013**, *7*, 3627−3634.
(47) Komaba, S.; Matsuura, Y.; Ishikawa, T.; Yabuuchi, N.; Murata, W.; Kuze, S. Redox reaction of Sn-polyacrylate electrodes in aprotic Na cell. *Electrochem. Commun.* **2012**, *21*, 65−68.
(48) Dai, K.; Zhao, H.; Wang, Z.; Song, X.; Battaglia, V.; Liu, G. Toward high specific capacity and high cycling stability of pure tin nanoparticles with conductive polymer binder for sodium ion batteries. *J. Power Sources* **2014**, *263*, 276−279.
(49) Farbod, B.; Cui, K.; Kalisvaart, W. P.; Kupsta, M.; Zahiri, B.; Kohandehghan, A.; Lotfabad, E. M.; Li, Z.; Luber, E. J.; Mitlin, D. Anodes for sodium ion batteries based on tin−germanium−antimony alloys. *ACS Nano* **2014**, *8*, 4415−4429.
(50) Zhu, H.; Jia, Z.; Chen, Y.; Weadock, N.; Wan, J.; Vaaland, O.; Han, X.; Li, T.; Hu, L. Tin anode for sodium-ion batteries using natural wood fiber as a mechanical buffer and electrolyte reservoir. *Nano Lett.* **2013**, *13*, 3093−3100.
(51) Han, X.; Liu, Y.; Jia, Z.; Chen, Y. C.; Wan, J.; Weadock, N.; Gaskell, K. J.; Li, T.; Hu, L. Atomic-layer-deposition oxide nanoglue for sodium ion batteries. *Nano Lett.* **2014**, *14*, 139−147.
(52) Qian, J.; Chen, Y.; Wu, L.; Cao, Y.; Ai, X.; Yang, H. High capacity Na-storage and superior cyclability of nanocomposite Sb/C anode for Na-ion batteries. *Chem. Commun.* **2012**, *48*, 7070−7072.
(53) Wu, L.; Hu, X.; Qian, J.; Pei, F.; Wu, F.; Mao, R.; Ai, X.; Yang, H.; Cao, Y. Sb-C nanofibers with long cycle life as an anode material for high-performance sodium-ion batteries. *Energy Environ. Sci.* **2014**, *7*, 323−328.
(54) He, M.; Kravchyk, K.; Walter, M.; Kovalenko, M. V. Monodisperse Antimony Nanocrystals for High-Rate Li-ion and Na-ion Battery Anodes: Nano versus Bulk. *Nano Lett.* **2014**, *14*, 1255−1262.
(55) Wu, L.; Lu, H.; Xiao, L.; Ai, X.; Yang, H.; Cao, Y. Electrochemical properties and morphological evolution of pitaya-like Sb@C micro-

DOI: 10.1021/acs.accounts.5b00482
Acc. Chem. Res. 2016, 49, 231−240

spheres as high-performance anode for sodium ion batteries. *J. Mater. Chem. A* **2015**, *3*, 5708−5713.
(56) Zhu, Y.; Han, X.; Xu, Y.; Liu, Y.; Zheng, S.; Xu, K.; Hu, L.; Wang, C. Electrospun Sb/C fibers for a stable and fast sodium-ion battery anode. *ACS Nano* **2013**, *7*, 6378−6386.
(57) Darwiche, A.; Marino, C.; Sougrati, M. T.; Fraisse, B.; Stievano, L.; Monconduit, L. Better cycling performances of bulk Sb in Na-ion batteries compared to Li-ion systems: An unexpected electrochemical mechanism. *J. Am. Chem. Soc.* **2012**, *134*, 20805−20811.
(58) Zhou, X.; Dai, Z.; Bao, J.; Guo, Y. G. Wet milled synthesis of an Sb/MWCNT nanocomposite for improved sodium storage. *J. Mater. Chem. A* **2013**, *1*, 13727−13731.
(59) Bodenes, L.; Darwiche, A.; Monconduit, L.; Martinez, H. The solid electrolyte interphase a key parameter of the high performance of Sb in sodium-ion batteries: comparative X-ray photoelectron spectroscopy study of Sb/Na-ion and Sb/Li-ion batteries. *J. Power Sources* **2015**, *273*, 14−24.
(60) Luo, W.; Lorger, S.; Wang, B.; Bommier, C.; Ji, X. Facile synthesis of one-dimensional peapod-like Sb@C submicron-structures. *Chem. Commun.* **2014**, *50*, 5435−5437.
(61) Li, Z.; Tan, X.; Li, P.; Kalisvaart, P.; Janish, M. T.; Mook, W. M.; Luber, E. J.; Jungjohann, K. L.; Carter, C. B.; Mitlin, D. Coupling In situ TEM and ex situ analysis to understand heterogeneous sodiation of antimony. *Nano Lett.* **2015**, *15*, 6339−6348.
(62) Kim, Y.; Park, Y.; Choi, A.; Choi, N. S.; Kim, J.; Lee, J.; Ryu, J. H.; Oh, S. M.; Lee, K. T. An amorphous red phosphorus/carbon composite as a promising anode material for sodium ion batteries. *Adv. Mater.* **2013**, *25*, 3045−3049.
(63) Qian, J.; Wu, X.; Cao, Y.; Ai, X.; Yang, H. High capacity and rate capability of amorphous phosphorus for sodium ion batteries. *Angew. Chem., Int. Ed.* **2013**, *52*, 4633−4636.
(64) Li, W. J.; Chou, S. L.; Wang, J. Z.; Liu, H. K.; Dou, S. X. Simply mixed commercial red phosphorus and carbon nanotube composite with exceptionally reversible sodium-ion storage. *Nano Lett.* **2013**, *13*, 5480−5484.
(65) Song, J.; Yu, Z.; Gordin, M. L.; Hu, S.; Yi, R.; Tang, D.; Walter, T.; Regula, M.; Choi, D.; Li, X.; Manivannan, A.; Wang, D. Chemically bonded phosphorus/graphene hybrid as a high performance anode for sodium-ion batteries. *Nano Lett.* **2014**, *14*, 6329−6335.
(66) Sun, J.; Lee, H. W.; Pasta, M.; Yuan, H.; Zheng, G.; Sun, Y.; Li, Y.; Cui, Y. A phosphorene−graphene hybrid material as a high-capacity anode for sodium-ion batteries. *Nat. Nanotechnol.* **2015**, *10*, 980−985.
(67) Baggetto, L.; Keum, J. K.; Browning, J. F.; Veith, G. M. Germanium as negative electrode material for sodium-ion batteries. *Electrochem. Commun.* **2013**, *34*, 41−44.
(68) Kohandehghan, A.; Cui, K.; Kupsta, M.; Ding, J.; Memarzadeh Lotfabad, E.; Kalisvaart, W. P.; Mitlin, D. Activation with Li enables facile sodium storage in germanium. *Nano Lett.* **2014**, *14*, 5873−5882.
(69) Su, D.; Dou, S.; Wang, G. Bismuth: A new anode for the Na-ion battery. *Nano Energy* **2015**, *12*, 88−95.
(70) Kim, I. T.; Allcorn, E.; Manthiram, A. High-performance FeSb-TiC-C nanocomposite anodes for sodium-ion batteries. *Phys. Chem. Chem. Phys.* **2014**, *16*, 12884−12889.
(71) Li, W.; Chou, S. L.; Wang, J. Z.; Kim, J. H.; Liu, H. K.; Dou, S. X. $Sn_{4+x}P_3$@ amorphous Sn-P composites as anodes for sodium-ion batteries with low cost, high capacity, long life, and superior rate capability. *Adv. Mater.* **2014**, *26*, 4037−4042.
(72) Kim, Y.; Kim, Y.; Choi, A.; Woo, S.; Mok, D.; Choi, N. S.; Jung, Y. S.; Ryu, J. H.; Oh, S. M.; Lee, K. T. Tin phosphide as a promising anode material for Na-ion batteries. *Adv. Mater.* **2014**, *26*, 4139−4144.
(73) Qian, J.; Xiong, Y.; Cao, Y.; Ai, X.; Yang, H. Synergistic Na-storage reactions in Sn_4P_3 as a high-capacity, cycle-stable anode of Na-ion batteries. *Nano Lett.* **2014**, *14*, 1865−1869.
(74) Xiong, H.; Slater, M. D.; Balasubramanian, M.; Johnson, C. S.; Rajh, T. Amorphous TiO_2 nanotube anode for rechargeable sodium ion batteries. *J. Phys. Chem. Lett.* **2011**, *2*, 2560−2565.
(75) Chen, C.; Wen, Y.; Hu, X.; Ji, X.; Yan, M.; Mai, L.; Hu, P.; Shan, B.; Huang, Y. Na^+ intercalation pseudocapacitance in graphene-coupled titanium oxide enabling ultra-fast sodium storage and long-term cycling. *Nat. Commun.* **2015**, *6*, 6929−6937.
(76) Qu, B.; Ma, C.; Ji, G.; Xu, C.; Xu, J.; Meng, Y. S.; Wang, T.; Lee, J. Y. Layered SnS_2-reduced graphene oxide composite - a high-capacity, high-rate, and long-cycle life sodium-ion battery anode material. *Adv. Mater.* **2014**, *26*, 3854−3859.
(77) Wu, L.; Lu, H.; Xiao, L.; Ai, X.; Yang, H.; Cao, Y. Improved sodium-storage performance of stannous sulfide@reduced graphene oxide composite as high capacity anodes for sodium-ion batteries. *J. Power Sources* **2015**, *293*, 784−789.
(78) Wu, L.; Lu, H.; Xiao, L.; Qian, J.; Ai, X.; Yang, H.; Cao, Y. A tin(ii) sulfide-carbon anode material based on combined conversion and alloying reactions for sodium-ion batteries. *J. Mater. Chem. A* **2014**, *2*, 16424−16428.
(79) Park, J.; Kim, J. S.; Park, J. W.; Nam, T. H.; Kim, K. W.; Ahn, J. H.; Wang, G.; Ahn, H. J. Discharge mechanism of MoS_2 for sodium ion battery: Electrochemical measurements and characterization. *Electrochim. Acta* **2013**, *92*, 427−432.
(80) Hu, Z.; Wang, L.; Zhang, K.; Wang, J.; Cheng, F.; Tao, Z.; Chen, J. MoS_2 nanoflowers with expanded interlayers as high-performance anodes for sodium-ion batteries. *Angew. Chem.* **2014**, *126*, 13008−13012.
(81) Lacey, S. D.; Wan, J.; Cresce, A. v. W.; Russell, S. M.; Dai, J.; Bao, W.; Xu, K.; Hu, L. Atomic force microscopy studies on molybdenum disulfide flakes as sodium-ion anodes. *Nano Lett.* **2015**, *15*, 1018−1024.
(82) Zhu, C.; Mu, X.; van Aken, P. A.; Yu, Y.; Maier, J. Single-layered ultrasmall nanoplates of MoS_2 embedded in carbon nanofibers with excellent electrochemical performance for lithium and sodium storage. *Angew. Chem., Int. Ed.* **2014**, *53*, 2152−2156.
(83) Xiong, X.; Luo, W.; Hu, X.; Chen, C.; Qie, L.; Hou, D.; Huang, Y. Flexible membranes of MoS_2/C nanofibers by electrospinning as binder-free anodes for high-performance sodium-ion batteries. *Sci. Rep.* **2015**, *5*, 9254.
(84) Zhao, L.; Zhao, J.; Hu, Y.-S.; Li, H.; Zhou, Z.; Armand, M.; Chen, L. Disodium terephthalate ($Na_2C_8H_4O_4$) as high performance anode material for low-cost room-temperature sodium-ion battery. *Adv. Energy Mater.* **2012**, *2*, 962−965.
(85) Park, Y.; Shin, D.-S.; Woo, S. H.; Choi, N. S.; Shin, K. H.; Oh, S. M.; Lee, K. T.; Hong, S. Y. Sodium terephthalate as an organic anode material for sodium ion batteries. *Adv. Mater.* **2012**, *24*, 3562−3567.
(86) Wang, S.; Wang, L.; Zhu, Z.; Hu, Z.; Zhao, Q.; Chen, J. All organic sodium-ion batteries with $Na_4C_8H_2O_6$. *Angew. Chem.* **2014**, *126*, 6002−6006.
(87) Luo, W.; Allen, M.; Raju, V.; Ji, X. An organic pigment as a high-performance cathode for sodium-ion batteries. *Adv. Energy Mater.* **2014**, *4*, 1400554.

DOI: 10.1021/acs.accounts.5b00482
Acc. Chem. Res. 2016, 49, 231−240